559-70

CHAIN DYNAMICS IN A DILUTE MAGNETORHEOLOGICAL FLUID

Jing Liu and Martin Hagenbuchle
Department of Physics and Astronomy
California State University Long Beach
Long Beach, CA 90840

ABSTRACT

The structure formation and dynamics of dilute, monodisperse ferrofluid emulsions in an external magnetic field have been investigated using dynamic light scattering techniques. In the absence of the magnetic field, the emulsion particles are randomly distributed and behave like hard spheres in Brownian motion. An applied magnetic field induces a magnetic dipole moment in each particle. Dipolar interaction between particles align them into chains where correlation function shows two decay processes. The short-time decay shows the motion of straight chains as a whole where the apparent chain length increases with the applied magnetic field and the particle volume fraction. Good scaling results are obtained showing that the apparent chain length grows with time following a power law with exponent of 0.6 and depends on the applied field, particle volume fraction and diffusion constant of the particles. The long-time decay in the correlation function shows oscillation when the chains reach a certain length with time and stiffness with threshold field. This result shows that chains not only fluctuate but move in a periodic motion with a frequency of 364 Hz at λ = 15. It may suggest the existence of phonons. This work is the first step in the understanding of the structure formation especially chain coarsening mechanism of MR fluids at higher volume fractions.

INTRODUCTION

Magnetorheological (MR) fluids are suspensions of magnetizable particles of roughly a micrometer in diameter in a non-magnetizable liquid. Without magnetic field, the particles are hard-sphere like and are in Brownian motion. An applied magnetic field induces a magnetic dipole moment in each particle. Dipolar interaction between particles align them into chains which may further coalesce to other larger structures. This microscopic structural transition changes viscosity dramatically and reversibly upon the removal of the field, leading to many potential applications from active shock absorbers and clutch controls for cars to seismic damage controls for bridges and buildings (Ref. 1). The key to these novel rheological properties are the structures induced by the applied magnetic field. While the goal of the research is to understand the mechanism of the structure formation of MR fluids, this work focuses on the initial stage of the structural transition: dynamic properties of chain formation in a dilute model MR fluid.

The dipolar interaction is anisotropic. It is attractive if the two dipoles is aligned within 55^0 relative to the applied field direction and it is repulsive if they are aligned outside this angle. When two dipoles are aligned head to tail with the field, the attractive force is the strongest. Thus if exposed to a magnetic field, the first reaction of randomly distributed dipoles is to form many separated chains. The chains then aggregates to form columns or worm-like wall structures depending on the volume fraction of the particles, the field strength and rate that was applied, and the sample geometry (Ref. 2-3). Theoretical calculation has shown that two-straight chains have a very short-range interaction which is typically two-particle diameters for our ferrofluid emulsion and the field applied (<400 G) (Ref. 4-5). However, we still observed the aggregation of chains to columns under this situation. A chain-fluctuation model for the chain-coarsening mechanism has been proposed by Halsey recently (Ref. 6). No one has quantitatively measured and studied the chain fluctuation.

In this paper we present the first measurement of chain formation and chain fluctuation with dynamic light scattering technique. We chose dilute MR fluids and weak applied fields to focus on the chain dynamics where no coarsening of the chains into columns occurs.

EXPERIMENTS

A ferrofluid emulsion (Ref. 7) was used as a model MR fluid. It consists of small ferrofluid droplets dispersed in water. The droplets are stabilized against irreversible aggregation and coalescence by the

surfactant *sodium dodecyl sulfate (SDS)*. The ferrofluid itself is a suspension of iron oxide grains in kerosene where the grains have an average diameter of 90 Å. Each of these grains possess a permanent dipole moment. Yet, there is no net dipole moment of the whole droplet since thermal motion keeps the orientation of the grains random. Only when an external magnetic field is applied, the grains orient and thus induce a dipole moment in each droplet which depends on the strength of the applied field. The distribution of droplet sizes in an emulsion is generally very broad. We obtained a monodisperse emulsion by applying the fractionated crystallization scheme which is described elsewhere (Ref. 8). Two particle sizes were used in the experiments with radius a: 233 ± 17 nm and 80 ± 24 nm measured by dynamic light scattering. The sample was diluted to a volume fraction in the range of $\phi \sim 10^{-4}$-10^{-6} to avoid multiple light scattering and chain coarsening.

We used an air-cooled Argon-ion laser at a wavelength of 514.5 nm and a He-Ne laser at 632.8 nm for our light scattering experiments. A lens was used to focus the laser beam into a cylindrical glass tube of 20 mm outer diameter which contained about 10 ml of the sample. This sample cell was surrounded by an index-match bath to reduce reflections and to keep the temperature of the sample constant. A Helmholtz coil with the sample in its center provided a homogeneous magnetic field. After passing the detector optics, the scattered light was detected by a photo-multiplier tube at different scattering angles in a plane normal to the field direction. The photon counts were then sent to a digital correlator (BI-9000AT) for processing, from which the averaged scattered light intensity I and the homodyne intensity autocorrelation function $\langle I(\tau)I(0)\rangle$ were obtained. Using the Siegert relation (Ref. 9) we converted the intensity autocorrelation function into the normalized field autocorrelation function $g^{(1)}(q,\tau) = \langle E(\tau)E(0)\rangle / \langle |E(0)|^2 \rangle$ from which the diffusion coefficients were derived as described below.

RESULTS

1. Chain Formation

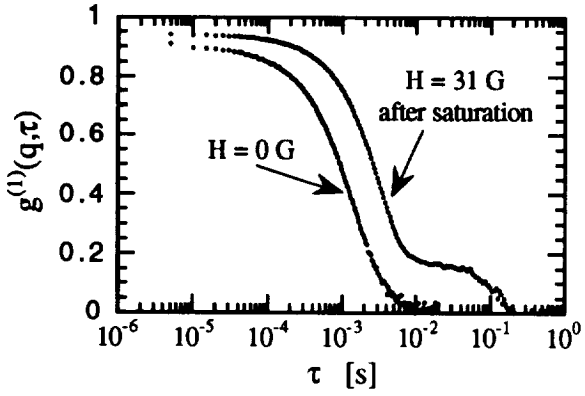

Fig. 1

Fig. 1. Normalized field autocorrelation function $g^{(1)}(q,\tau)$ without magnetic field ($H = 0$) and after saturation ($H = 31$ G, $\lambda = 9.4$, t=110 min.). Here particle radius a=233 nm, Scattering angle $\theta = 90^0$, and volume fraction $\phi = 7.65 \times 10^{-5}$.

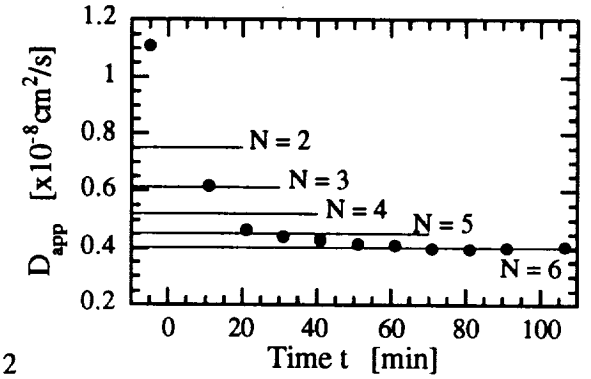

Fig. 2

Fig. 2. Short-time self diffusion coefficient during chain formation at H = 31 G for the same conditions as in Fig. 1. The constant levels are calculated diffusion coefficients for a chain consisting of N particles.

Fig. 1 shows the comparison of the normalized field autocorrelation function $g^{(1)}(q,\tau)$ at applied magnetic field $H = 0$ G and $H = 31$ G for $\phi = 7.7 \times 10^{-5}$, a = 233 nm and scattering angle $\theta = 90^0$. The correlation function with applied magnetic field was measured after the chain formation had stopped which means after the scattered intensity $I(t)$ had saturated. The differences between the two correlation functions is clearly shown in Fig. 1. The correlation function at zero field can essentially be described by a single exponential. Due to the high dilution the emulsion behaves like a system of non-interacting particles. The small deviation from an exponential function is caused by the small size polydispersity of the droplets. In contrast, $g^{(1)}(q,\tau)$ with applied magnetic field decays generally slower and shows two distinct decay times at

H=31G. At this field, the dipolar interaction energy between two dipoles in contact is 9.4 time of the thermal energy, i.e. the coupling constant λ = 9.4. The main decay time at this earlier time is of the same order of magnitude as the zero-field decay time. Compared to this short-time decay the long-time decay is about two orders of magnitude slower.

In the following we focus only on the short-time behavior of $g^{(1)}(q,\tau)$. The short-time dynamics is usually described in terms of the first cumulant $\Gamma_1(q)$ (Ref. 10):

$$\Gamma_1(q) = -\frac{\partial}{\partial\tau} \ln g^{(1)}(q,\tau)\Big|_{\tau=0} \qquad (1).$$

The first cumulant defines an apparent diffusion coefficient through:

$$\Gamma_1(q) = q^2 D_{app}(q) \qquad (2).$$

Therefore, $D_{app}(q)$ can be obtained from Fig. 1 using Eqs. 1 and 2. In general $D_{app}(q)$ contains both self and collective diffusion. However, there are two arguments that in our experiment $D_{app}(q)$ is solely determined by the self diffusion of the particles. First, since the threshold distance, which is a measure of the magnetic interaction range, is about two-particle diameters (2a) and the dilution is so high that the initial distance d_i between neighboring particles are about 20 x 2a, after saturation we have essentially a system of non-interacting chains. Without interaction there are no correlations between different chains. Thus, $D_{app}(q)$ reduces to $D_{app}^{self}(q)$. Second, it has been pointed out by several authors (Ref. 10-11) that for $q >> q_{max}$, $D_{app}(q)$ reduces to $D_{app}^{self}(q)$ even in interacting colloidal suspensions. Here, $q_{max} = 2\pi/d_{max}$ with d_{max} the nearest neighbor distance between chains and $q = 2\pi/l_q$ is the scattering wavevector employed in our experiment where l_q = 273 nm ~ 2a. Since $d_{max} >> l_q$, the above mentioned condition $q >> q_{max}$ is well fulfilled.

Figure 2 shows $D_{app}^{self}(q)$ during the chain formation for the same sample as the one used in Fig. 1. The magnetic field was switched on at time 0 and kept constant at 31 G. The time to measure a correlation function was two minutes. The first and the last point in Fig. 2 correspond to the two correlation functions presented in Fig. 1. The diffusion coefficient of a chain of particles decreases with increasing number of particles in the chain. Thus, Fig. 2 directly reflects the chain formation. Due to our scattering geometry where the scattering wavevector is normal to the field direction, we are sensitive only to the motion of the chains perpendicular to their axes. Using the Stokes Einstein relation and the appropriate friction coefficient $F_{chain}^{\perp}$ (Ref. 12), we can calculate the diffusion coefficient $D_{chain}^{\perp}$ normal to the field direction:

$$D_{chain}^{\perp} = \frac{k_B T}{F_{chain}^{\perp}}, \qquad F_{chain}^{\perp} = \frac{4N}{3\ln 2N + \gamma^{\perp}} \cdot F_{sphere} \qquad (3).$$

Here, F_{sphere} is the Stokes friction coefficient of a single particle, N is the number of particles in the chain, and for $\gamma^{\perp}$ a value of - 0.418 was reported (Ref. 13). The calculated values for N = 2 to 6 are presented in Fig. 2 as constant levels. Comparing the diffusion coefficients calculated from Eq. 3 with the extrapolated values from measurements based on Eq. 1-2, we can estimate the apparent number of particles in an average chain. We find that at saturation the chain consists of approximately six particles. Here we do not expect one single chain length but a distribution of chain lengths to be induced by the applied field. Therefore the diffusion coefficient we measure is actually an averaged diffusion coefficient corresponding to an average chain length. The estimate for the number of particles in a chain from Eq. 3 is based on straight chains in the sample. Therefore, we call it apparent chain length. In reality, dynamic light scattering is

sensitive to all kinds of motion. Thus if there are bending modes or chain fluctuations as we will show later, they will affect $D_{app}^{self}(q)$ to some degree.

2. Influence of Applied Field and Volume Fraction on Short-Time Dynamics

If we increase the field strength, the interaction range between particles will increase. This leads to the formation of longer chain lengths. Therefore, the measured diffusion coefficient at short time will be reduced. Figure 3 shows the growth of the apparent chain lengths with time at different fields from 52 to 195 G corresponding to λ = 26 to 228. The same sample as in Fig. 1 was used with $\phi = 1.4 \times 10^{-5}$ and $\theta = 90^0$ using He-Ne laser of wavelength 632.8 nm. When the field is ramped up quickly and held at a constant value, the short-time self diffusion coefficient similar to Fig. 2 is observed which decreases with time as chains build up. The stronger the applied field, the faster the diffusion coefficient decreases, and therefore, a longer chain length is formed. The apparent chain length is obtained the same way as the one in Fig. 2 by comparing calculated diffusion coefficient for straight chains with experimental data.

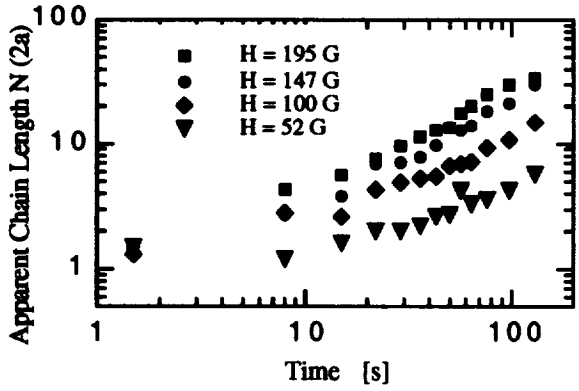

Fig.3

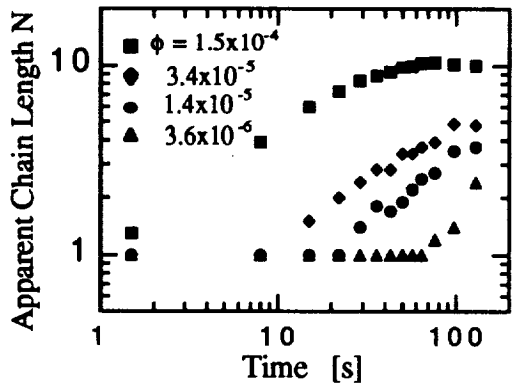

Fig.4

Fig. 3. Apparent chain length in units of particle diameters vs. time measured for different applied field strengths which correspond to λ = 26, 85, 156, 228. The field is turned on at t=0. $\phi = 1.4 \times 10^{-5}$.

Fig. 4. Apparent chain length vs. time measured for different particle volume fractions at H=50 G and λ=24. Both figures correspond to a=233 nm and $\theta = 90^0$.

Figure 4 shows the results of changing particle volume fractions for the same sample at a constant field of 50 G (λ=24) and $\theta = 90^0$ using Ar^+ laser of wavelength 514.5 nm. If we increase the particle volume fraction ϕ, the initial distance between particles is reduced which shortens the diffusion time for particles to enter each other's interaction range which is defined by $\lambda \geq 1$ and more particles are within that range to form chains. Therefore, a longer chain is formed as compared to that at low ϕ for the same time after the field is applied. Specifically, at $\phi = 3.6 \times 10^{-6}$, a dimer forms after the field is turned on for one hour. Whereas at $\phi = 1.5 \times 10^{-4}$, it takes only 1 minute. However, they both increase with time at a similar rate on this log-log scale once dimers are formed and N starts to increase. The slowing down of N at $\phi = 1.5 \times 10^{-4}$ at later time might be due to the sedimentation of long chains and the long-time decay influence to the short-time behavior in the correlation function. The ferrofluid emulsion is nearly density matched but not exactly. When chain gets longer, sedimentation becomes more obvious.

Figure 5 shows the apparent chain length from Fig. 3 and 4 plotted as a function of rescaled time on a log-log scale. The normalization factor is a characteristic time scale, t_{BW}, for particles to aggregate. This time factor originates from the Brownian motion weighted by the stability factor W to take into account of dipolar interaction: $t_{BW} = t_B W = 9.16\ a^2/(6D\phi\lambda^{4/3})$ (Ref. 14). All the data collapse to follow a power law $N = (t/t_{BW})^z$ where z=0.6 as shown in Fig. 5. For $\lambda \geq 9$, the aggregation process is non-equilibrium or irreversible for the

volume fractions used in our experiments (Ref. 15). At lower H or ϕ, it takes a longer time for two particles to move into each other's interaction range to form a dimer. However, the growth rate of average chains for each sample measured follows the same relation: $dN/dt \sim \lambda^{0.8}\phi^{0.6}D^{0.6}t^{-0.4}$. The larger the interaction strength and diffusion constant or the closer the initial particle distance, the faster the chains grow.

A power-law behavior shows that the chain formation can be described by the Smoluchowski's equation for irreversible aggregation. It means that the formation of a N-particle chain is due to a combination of two short chains at any given time. Earlier study of ER fluid by Fraden et al. has shown a similar behavior with z =0.6 (Ref. 16).

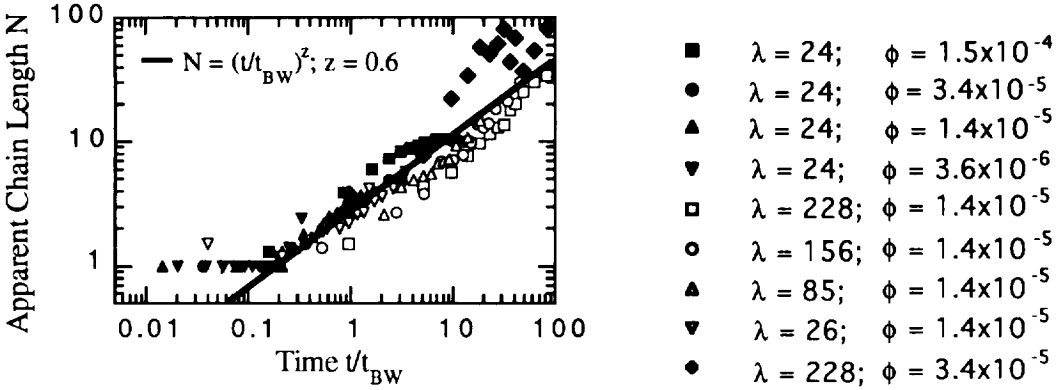

Fig. 5. Apparent chain length in units of particle diameter vs. normalized time for the data shown in Fig. 3 and 4. All the measurements show the same power-law growth.

3. Long-Time Dynamics

Figure 1 shows that an additional decay appears at long time when the field is applied. As the short time decay reflects the diffusing motion of a straight chain, the long time decay may reflect additional motion of a chain. On a closer look at the long-time behavior one finds surprising results. Figure 6 shows correlation functions measured at different angles when the same field is turned on for about two hours. In this case, smaller size particles with a=80 nm are used at a higher field (H=310 G and λ = 15) than that used in Fig. 1. Now an average chain consists of about 300 particles which is at least a factor of 10 more than the particles in a typical chain formed with larger particles used in obtaining Fig. 1-4. A little bump at the decay slope in Fig. 6a indicates that an additional motion may exist and overlaps with the short-time decay. Dramatic results are seen at the scattering angle of 150^0 where oscillation is observed. The first oscillation peak of the correlation function in Fig. 6b occurs at a time about 2.7 ms which corresponds to a frequency of 364 Hz. Oscillation in the correlation function indicates that chains fluctuate regularly at this characteristic frequency. If plotted in a linear scale, the interval between oscillations are constant. This shows the possibility of existence of phonons which is surprising to see in a heavily damped system.

The differences between Fig. 6a and 6b is the length scale or window used to measure transverse motion: $l_q = 1/q = 1.5 \times 2a$ for $\theta = 150^0$, whereas $l_q = 2.1 \times 2a$ for $\theta = 90^0$. This indicates that the fluctuation amplitude, A_f, is about two-particle diameters. If $l_q > A_f$, the fluctuation is averaged out as seen by the detector. If $l_q < A_f$, the fluctuation can be detected. This observation is consistent with other measurements at smaller angles of 30^0 and 60^0 where the bump becomes less obvious.

The oscillation does not occur at all the times. It appears about 15 minutes after the field is turned on which depends on the field applied, the particle volume fractions, and the particle size. The oscillation amplitude increases and the peak width narrows down with time. If we reduce the field step by step after saturation is reached, the oscillation in the correlation function generally reduces with field and disappears at low field where no chain exists. Thus a certain threshold-field strength is required to see oscillation. This

indicates that a certain length and stiffness of chains is required to support oscillation. It is consistent with the picture of phonon propagating along a chain in a damped environment.

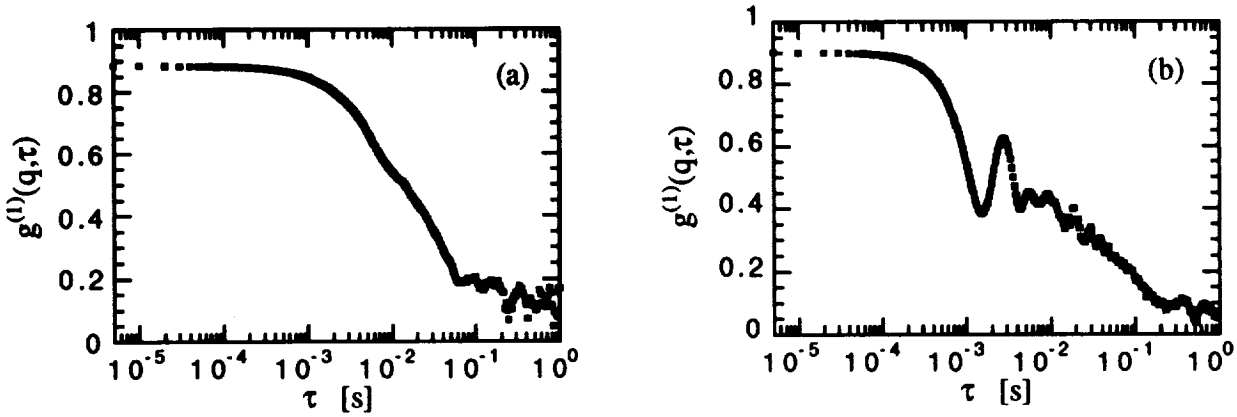

Fig. 6. Correlation function measured at scattering angles of (a) 90^0 and (b) 150^0 corresponding to a length scale l_q=1/q= 2.1 x 2a and 1.5 x 2a. Oscillation is observed and becomes pronounced at 150^0. Here H=310G (λ = 15) , ϕ=3.6 x 10^{-5}, a =80 nm.

CONCLUSION

In summary, we have presented initial dynamic-light-scattering measurements on a dilute model magnetorheological fluid. Field-induced chain formation was observed for $\lambda > 1$. The motion of chains can be described by two processes: the diffusive motion of straight chains as a whole and the fluctuation of chains. The straight-chain motion corresponds to a diffusion constant which decreases with the increase of applied field and particle volume fraction. The chain fluctuation shows a surprising periodic oscillation at a time scale of a few ms when the chains reach a certain length with time and stiffness at a threshold field. This result may suggest the existence of phonons along chains. The observed chain fluctuation supports the basis of Halsey's theory for the chain-coarsening mechanism.

ACKNOWLEDGMENT

We thank Dr. Yun Zhu and Dr. Mark Gross for helpful discussion and gratefully acknowledge the support by NASA, NAG 3-1634.

REFERENCES

1. J. D. Carlson, et al, *Proc. of 5th Int. Conf. on Electro-Rheological Fluids and Magneto-Rheological Suspensions,* University of Sheffield, UK, 10 - 14 July 1995, Bullough ed. (World Scientific, 1996).
2. E.M. Lawrence, et al, *Int. J. Mod. Phys. B,* **8**, 2765 (1994).
3. J. Liu, et al, *Phys. Rev. Lett.* 74, 2828 (1995).
4. R. Tao and J. M. Sun, *Phys. Rev. Lett.* **67**, 398 (1991).
5. B. Murakami, APS March Meeting, St. Louis, 1996.
6. T.C. Halsey and W. Toor, *J. Stat. Phys.*, **61**, 1257 (1990).
7. J. Bibette, *J. Magnetism and Magn. Materials* **122** (1993) 37.
8. J. Bibette, *J. Coll. Int. Sci.* **147** (1991) 474.
9. B. J. Berne and R. Pecora, *Dynamic Light Scattering* (Wiley, New York, 1976).
10. P. N. Pusey, *J. Phys. A: Math. Gen.* **11** (1978) 119.
11. K. J. Gaylor, I. K. Snook, W. J. van Megen, and R. O. Watts, *J. Phys. A: Math. Gen.* **13** (1980) 2513.
12. K. Zahn, R. Lenke, and G. Maret, *J. Phys. II France* **4** (1994) 555.
13. H. Yamakawa, *J. Chem. Phys.* **53** (1970) 436.
14. M. Fermigier and A. P. Gast, *J. Coll. Int. Sci.* **154** (1992) 522.
15. P. G. de Gennes and P. Pincus, *Phys. Kondes, Mater.* **11**, 189 (1970).
16. S. Fraden, A. J. Hurd, and R.B. Meyer, *Phys. Rev. Lett.* 63, 2373 (1989).